

Oct 14th, 12:00 AM

## Experimental Response of Connections Between Cold-formed Steel Profile and Cement-based Panel

Luigi Fiorino

Ornella Iorio

Raffaele Landolfo

Follow this and additional works at: <https://scholarsmine.mst.edu/isccss>



Part of the [Structural Engineering Commons](#)

---

### Recommended Citation

Fiorino, Luigi; Iorio, Ornella; and Landolfo, Raffaele, "Experimental Response of Connections Between Cold-formed Steel Profile and Cement-based Panel" (2008). *International Specialty Conference on Cold-Formed Steel Structures*. 8.

<https://scholarsmine.mst.edu/isccss/19iccfss/19iccfss-session9/8>

This Article - Conference proceedings is brought to you for free and open access by Scholars' Mine. It has been accepted for inclusion in International Specialty Conference on Cold-Formed Steel Structures by an authorized administrator of Scholars' Mine. This work is protected by U. S. Copyright Law. Unauthorized use including reproduction for redistribution requires the permission of the copyright holder. For more information, please contact [scholarsmine@mst.edu](mailto:scholarsmine@mst.edu).

## **Experimental response of connections between cold-formed steel profile and cement-based panel**

Luigi Fiorino<sup>1</sup>, Ornella Iuorio<sup>2</sup>, Raffaele Landolfo<sup>2</sup>

### **ABSTRACT**

The seismic response of sheathed cold-formed steel (CFS) structures is highly influenced by the shear behaviour of panel-to-steel framing connections. Therefore, an experimental campaign aiming at characterizing the shear behaviour of different sheathing-to-CFS profiles connections has been planned. In particular, the following objectives have been selected: to compare the response of different panel typologies (cement, wood and gypsum-based panels); to examine the effect of the loaded edge distance; to investigate the outcome of different cyclic loading protocols. This paper presents and discusses the main results of this experimental investigation carried out on cement-based sheathing-to-stud connections.

### **Introduction**

The wide development of light gauge steel structures in the housing market increases the interest in searching new solutions and materials able to satisfy different market demands. Moreover, the new materials should be able to guarantee structural and environmental performance equal or higher than which provided by common materials.

<sup>1</sup>Department of Structural Engineering, University of Naples "Federico II", Naples, Italy

<sup>2</sup> Department of Constructions and Mathematical Methods in Architecture, University of Naples "Federico II", Naples, Italy

For these reasons, taking into account that in CFS studs structures the skeleton is usually sheathed with metal sheets, sandwich panels, wood-based or gypsum-based panels, the presented research has been aimed to investigate the behaviour of screw connections between CFS profiles and cement-based panels. In particular, the used panels (“Placocem” Fig. 1) are produced by BpB Italia Spa and are made of a cement core lightened with polystyrene and reinforced with a net of mineral fibers on both sides.



Figure 1: Placocem by BpB Italia Spa

When the sheathing has adequate strength and stiffness and it is effectively connected with the skeleton, then the interaction between profiles, sheathings and connections can be advantageously taken into account in the structural analysis (“sheathing-braced” design). In this case, the sheathing positively affects the structural response under vertical and horizontal loads. In particular, in case of gravity loads, the presence of sheathings can be advantageously taken into account in predicting the compression strength of vertical studs. This strength, in fact, may be significantly increased as a result of the additional resistance provided by the sheathing against global buckling modes. Hence, in current structural codes (AISI, 2002, EN 1993-1-3), it is allowed to take into account this member-to-sheathing interaction by using semi-empirical calculations based on the interpretation of test results. In the case of horizontal loads, floors, roof and walls can perform as diaphragms forming a “box system”. In particular, floors and roofs can be considered simply supported diaphragms, whereas walls can be regarded as vertical, cantilevered diaphragms. The “sheathing-braced” design approach requires the structural analysis of sheathings, connections, diaphragm edge members and tie-down connections to be carried-out. Despite the strong interrelation between the global lateral response of sheathed cold-formed “stick-built” structures and the local behaviour of sheathing-to-stud connections, few experimental programs have been carried out to study the response of sheathing to stud connections subjected

to shear loads (Filipsson, 2002, Fulop and Dubina, 2004, Okasha, 2004). For this reason, a specific experimental research has been planned, aiming to investigate both the monotonic and cyclic shear capacity of screw connections between CFS profiles and wood, gypsum or cement-based sheathings.

This paper is focused on cement-based sheathing-to-stud connections tests, and refers to Fiorino et al., 2007 for the experimental campaign on wood and gypsum-based panels. This study is part of a more comprehensive research program, devoted to analyzing the behaviour of light-gauge steel low-rise residential buildings under seismic actions (Landolfo et al., 2006)

### **The experimental program**

The experimental program was organized in two phases: in a first phase connections between studs and wood or gypsum-based panels were tested and in a second phase fasteners between studs and cement-based panels were tested. Goal of the testing program was: (1) to compare the response of different panels typologies (wood, gypsum and cement-based panels); (2) to examine the effect of the distance from the centre of the screw to the adjacent edge of the connected part in the direction parallel to the load transfer (loaded edge distance); (3) to evaluate the effect of different cyclic loading protocols; (4) to study the effect of sheathing orientation (only for the case of wood-based panels); (5) to assess the effect of the loading rate. This paper is focused on the second phase and it refers to Fiorino et al., 2007 for the first phase. Therefore, it is worth to specify that in the second phase only the first three points were tests goals, whilst orientation and effect of loading rate were not studied. Hence, 32 specimens, grouped in 8 series composed of 4 nominally identical specimens were tested. For each series, the experimental results were assumed as average values of single specimen results.

Test setup, geometry and materials properties of specimens were fixed during all the experimental campaign (Fig. 2). In particular, the generic sheathing-to-profile connection specimen consisted of two single  $200 \times 600$  mm sheathings attached to the opposite flanges of CFS profiles. Steel profiles were made of  $100 \times 50 \times 10 \times 1.0$  mm C (lipped)-sections. In particular, one single C-section was placed on the top side, whereas two back-to-back coupled C-sections were used for the bottom side. The profiles were fabricated from S350 hot dipped galvanized (zinc coated) steel (nominal yield strength  $f_y = 350$  MPa; nominal tensile strength  $f_t = 420$  MPa). The CFS profiles were bolted to hot-rolled steel (HRS) T-sections used to connect the specimens to the universal testing machine. Moreover, in order to avoid significant web deformation of the CFS profiles, a steel plate was placed at the internal side of the web of both top and

bottom studs. Three different sheathing types were selected: 9.0 mm thick type 3 oriented strand board (OSB) (EN 300, 1997), 12.5 mm thick standard gypsum wallboard (GWB, ISO-6308, 1980) and 12.5 mm thick cement based boards. In particular, taking into account that the OSB panels are composed of wood strands oriented along a principal direction, two different configurations were investigated: boards with strands in direction parallel to the applied loads (OSB//) and boards with strands in direction perpendicular to the applied loads (OSBT). Sheathings were connected using three screws (spaced at 150 mm on centre) for the top member (tested connections) and two rows of eight screws (spaced at 75 mm on centre) for the bottom members (oversized connections). Appropriate fasteners for each sheathing typology were adopted:  $4.2 \times 25$  mm (diameter  $\times$  length) flat head self drilling screws for OSB sheathings, and  $3.5 \times 25$  mm bugle head self drilling screws for CP and GWB panels. Four linear variable differential transducers (LVDTs) were used to measure the displacement between the sheathing and the profile.

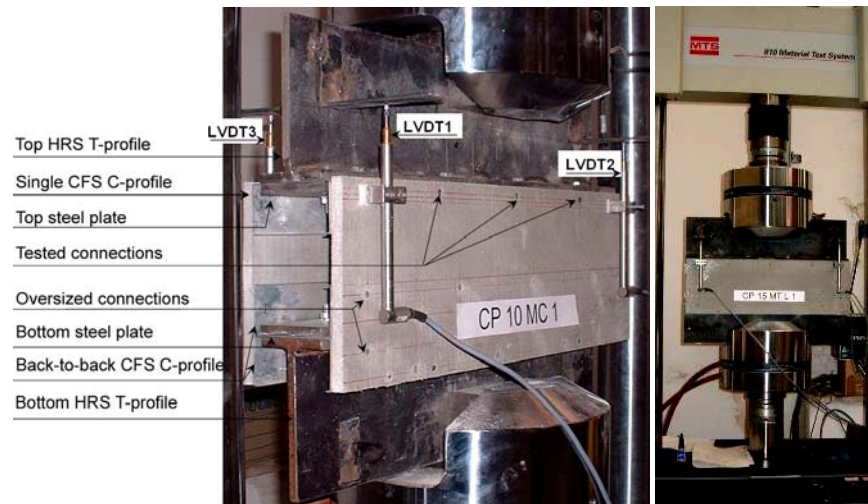


Figure 2: Generic specimen.

Three different values of the loaded edge distance ( $a$ ) were adopted ( $a = 10$  mm,  $a = 15$  mm,  $a = 20$  mm). The cyclic tests were carried out on specimens having  $a = 20$  mm. In this second phase of the experimental campaign, four displacement-controlled test procedures were adopted: monotonic tension (MT series), monotonic compression (MC series), and two types of cyclic loading history (labeled as CF and CK series). Under the monotonic loading history, specimens were subjected to progressive displacements, without unloading

phases. In the cyclic tests, two different loading protocols were adopted. In the first protocol (CF), specimens were subjected to specific loading sequences based on the results of a numerical study on the probable deformation demand from typical Italian earthquakes (Della Corte et al., 2006). In this case, specimens were tested with a constant loading rate. The second loading procedure (CK) was the CUREE protocol for ordinary ground motions (Krawinkler H, et al., 2000). It was developed to represent the seismic demand on wood framed shear walls under typical Californian earthquakes. In this case, specimens were tested with a constant cyclic frequency of  $f = 0.20$  Hz. The displacement history for each adopted loading protocol is shown in Figure 3, in which the applied displacements ( $d$ ) are normalized with respect to the reference displacement ( $\Delta$ ). The definition of the reference displacement is different for CF and CK protocols. In particular, the reference displacement is related to the yield displacement for CF procedure ( $\Delta=0.91\text{mm}$ ), while it is based on the measure of the ultimate displacement for the CK protocol ( $\Delta=4.17\text{mm}$ ). Specimens were tested with loading rate ( $v$ ) of  $0.05$  mm/s for monotonic tests,  $0.5$  mm/s for CF cyclic tests. The whole test program is summarized in Table 1, where the variables under investigation are reported for each series.

Serie Label	a (mm)	Loading protocol	Loading direction	Loading rate $v$ (mm/s)	Number of specimens
CP10MT	10	Monotonic	Tension	0.05	4
CP10MC	10	Monotonic	Compression	0.05	4
CP15MT	15	Monotonic	Tension	0.05	4
CP15MC	15	Monotonic	Compression	0.05	4
CP20MT	20	Monotonic	Tension	0.05	4
CP20MC	20	Monotonic	Compression	0.05	4
CP20CK	20	Cyclic	-	Variable	4
CP20CF	20	Cyclic	-	0.5	4

Table 1: Test program matrix

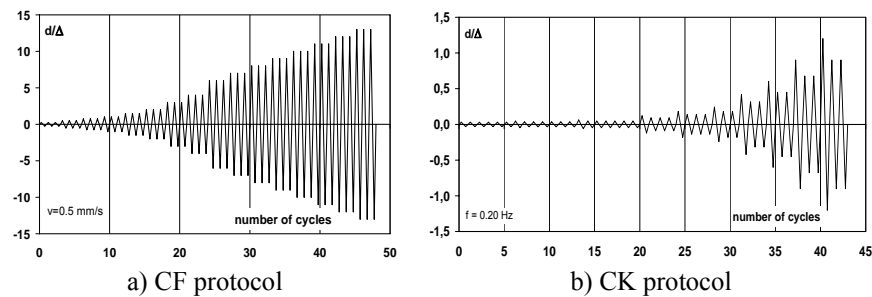


Figure 3: Loading protocols

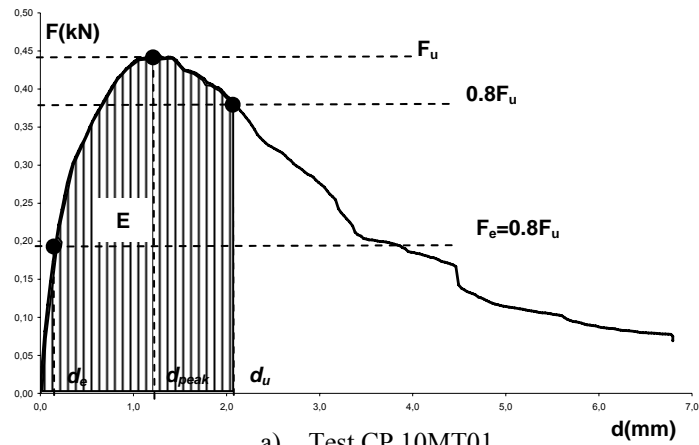
The series label defines both the specimen typology and testing procedure. Namely, the first group of characters indicates the sheathing material (CP: cement-based board); the second group of characters represents the loaded edge distance measured in millimeters (10, 15, or 20 mm); the third group describes the loading protocol (MT, MC, CF or CK). For example, the label CP 10 MT refers to a specimen made with cement-based panels, with edge distance equal to 10 mm, submitted to monotonic tension test.

### Test results

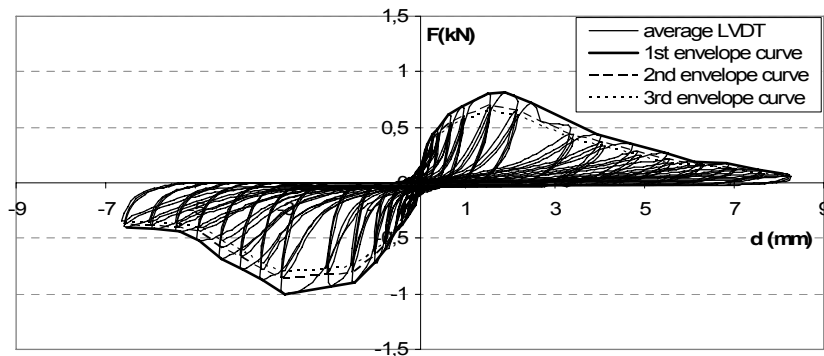
Typical experimental responses obtained in monotonic and cyclic tests are shown in Figure 4. Parameters used to describe the experimental behaviour are:

- $F = F_{tot}/6$ : average screw load ( $F_{tot}$  is the total recorded load, 6 is the total number of screws);
- $d = (d_{LVDT1} + d_{LVDT2} + d_{LVDT3} + d_{LVDT4})/4$ : average displacement ( $d_{LVDTi}$  is the displacement recorded by the  $i^{\text{th}}$  LVDT);
- $F_u$ : strength, is the maximum recorded average load;
- $d_{peak}$ : displacement corresponding to  $F_u$ ;
- $F_e = 0.4F_u$ : conventional elastic strength;
- $d_e$ : displacement corresponding to  $F_e$ ;
- $K_e = F_e/d_e$ : conventional elastic stiffness;
- $d_u$ : displacement corresponding to a load equal to  $0.80F_u$  on the post-peak branch of response;
- $\mu = d_u/d_e$ : maximum ductility;
- $E$ : absorbed energy (area under the  $F$  vs.  $d$  curve for  $d \leq d_u$ ).

In the case of cyclic tests these parameters are defined both on the positive and negative envelope curves, the latter defined considering the first hysteretic loops (Fig. 4(b)). Monotonic and cyclic test results are summarized in Table 2.



a) Test CP 10MT01



b) Test CP 20 CF 02

Figure 4: Typical experimental response

In this Table the parameters used to describe the experimental behaviour are reported together with the observed failure mode. For the cyclic tests, average values of parameters obtained on the positive and negative first envelope curves are reported.

In particular, the observed failure mechanisms during monotonic tests were (Fig. 5):

- (T) tilting of screws (Fig. 5(b));
- (P) screws pull-through the sheathing (Fig. 5(b));
- (E) breaking of sheathing edge (Fig. 5(a));

where tilting of screws was always observed in combination with the other mechanisms.



Specimen	$K_e$ (kN/mm)	$F_e$ (kN)	$d_e$ (mm)	$F_u$ (kN)	$d_{peak}$ (mm)	$d_u$ (mm)	$E$ (kNxmm)	$\mu$	Failure mode
CP 10 MT 0	2.77	0.17	0.06	0.42	1.11	2.01	0.74	33.32	E
CP 10 MT 1	1.98	0.18	0.09	0.44	1.09	2.08	0.79	23.09	E
CP 10 MT 2	4.61	1.56	0.03	0.39	0.33	1.19	0.40	35.38	E
CP 10 MT 3	2.34	0.19	0.08	0.48	0.65	2.17	0.92	26.52	E
CP 15 MT 1	2.48	0.20	0.08	0.51	0.90	2.95	1.32	36.07	E
CP 15 MT 3	3.45	0.25	0.07	0.62	1.31	1.88	1.05	26.32	E
CP 15 MT 4	2.46	0.25	0.10	0.62	1.35	2.17	1.16	21.49	E
CP 15 MT 5	3.18	0.24	0.07	0.59	1.29	1.90	1.01	25.67	E
CP 20 MT 2	2.42	0.29	0.12	0.73	1.66	3.46	2.20	28.50	T+P+E
CP 20 MT 3	3.20	0.27	0.09	0.68	1.63	2.72	1.62	31.91	T+P+E
CP 20 MT 4	3.20	0.36	0.11	0.91	1.83	2.47	1.89	21.82	E
CP 20 MT 5	2.91	0.31	0.11	0.78	2.30	3.54	2.37	32.87	E
CP 10 MC 1	1.56	0.54	0.35	1.36	1.97	3.44	3.73	9.90	T+P
CP 10 MC 2	2.22	0.37	0.17	0.92	2.46	9.33	7.52	56.44	T+P+E
CP 10 MC 3	1.59	0.37	0.23	0.93	2.08	7.45	6.02	31.80	T+E
CP 10 MC 4	0.87	0.40	0.46	0.99	2.84	9.12	7.39	20.02	T+E
CP 15 MC 1	3.47	0.54	0.16	1.35	4.52	6.61	7.73	42.41	T+P
CP 15 MC 2	0.73	0.53	0.73	1.33	6.37	6.89	6.82	9.45	T+P
CP 15 MC 3	1.31	0.52	0.39	1.29	5.50	0.52	8.84	20.14	T+P
CP 15 MC 4	1.25	0.51	0.40	1.26	5.33	6.88	7.12	17.07	T+P
CP 20 MC 1	1.93	0.57	0.30	1.43	4.10	6.09	7.22	20.57	T+P
CP 20 MC 2	0.86	0.62	0.73	1.56	6.53	8.32	10.04	11.44	T+P
CP 20 MC 3	1.29	0.64	0.50	1.60	6.54	8.18	10.34	16.52	T+P
CP 20 MC 4	1.22	0.60	0.49	1.50	4.70	5.20	5.70	10.61	T+P
CP20 CK 01	0.93	0.36	0.41	0.89	2.72	4.55	3.33	11.63	P+E
CP 20 CK 02	1.08	0.44	0.44	1.09	2.61	4.75	4.12	12.42	P+E
CP 20 CK 03	2.09	0.41	0.20	1.03	2.52	4.44	3.77	23.50	P+E
CP 20 CK 04	2.90	0.38	0.18	0.95	2.17	3.90	3.19	28.37	P+E
CP 20 CF 01	1.95	0.39	0.27	0.97	1.98	3.15	2.46	15.78	T+E
CP 20 CF 02	1.57	0.35	0.30	0.91	2.41	3.36	2.47	14.23	T+P+E
CP 20 CF 03	1.85	0.31	0.17	0.79	1.51	3.31	2.19	19.86	T+P+E
CP 20 CF 04	2.37	0.32	0.12	0.81	1.63	3.41	2.47	26.90	T+P+E

Table 2: Experimental results of monotonic and cyclic tests.

The most common mechanism observed during monotonic tension tests was the breaking of the sheathing edge ((E) failure mode), except for CP20MT2 and CP20MT3, where combination of tilting of screws, screws pull-through the sheathing and breaking of sheathing edge occurred ((T)+(P)+(E) failure mode). On the other side, in the monotonic compression tests the failure mechanism was a combination of tilting of screws and screws pull-through the sheathing ((T)+(P) failure mode), except for CP10MC3 and CP10MC4 in which the combination of tilting of screws and breaking of sheathing edge occurred ((T)+(E) failure mode). In addition, in one case the combination of three failure modes was observed: (T)+(P)+(E) for CP10MC2.

In the case of cyclic loading characterized by CK protocol, combination of screw pull-through the sheathing and breaking of sheathing edge ((P)+(E) failure mode) was the dominant mechanism. Whilst, in case of CF protocol, the combination of all the failure mechanisms (T)+(P)+(E) was observed in all the tests except for CP20CF1 when only a combination of tilting of screws and breaking of sheathing edge (T)+(E) developed.

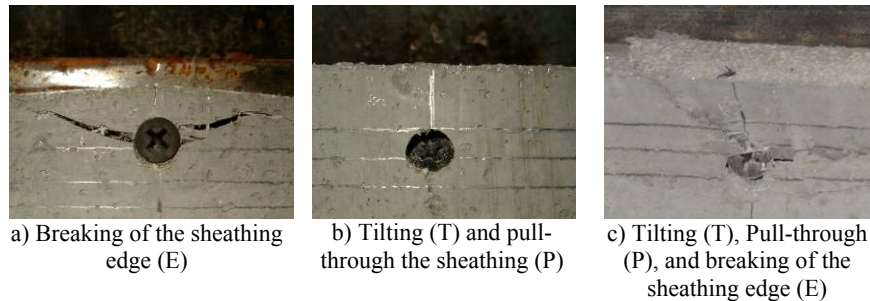


Figure 5: Test program matrix

### Effect of the sheathing type

Monotonic experimental results obtained for OSB//, OSBT, GWB and CP tests are illustrated in Figure 6. In particular, in this Figure the average values of  $K_e$  (Fig. 6(a)),  $F_u$  (Fig. 6(b)),  $\mu$  (Fig. 6(c)), and  $E$  (Fig. 6(d)) concerning to the monotonic tension (MT) and compression (MC) tests are represented as functions of the loaded edge distance ( $a$ ). Examining these figures, it can be noted that connections with CP sheathings revealed larger stiffness than any other material, with on average, values 1.6, 2.1 and 3.4 times larger than that showed by GWB, OSB// and OSBT panels, respectively. Moreover, the ductility revealed by CP was, on average 2.2 and 2.3 times larger than that showed by OSB// and OSBT panels, but 1.1 lower than that exhibited by GWB panels. On the contrary, CP panels showed less strength and absorbed energy than connections with OSB// and OSBT sheathings (on average, the strength was 2.0 and 2.3 times lower and the absorbed energy of CP panels was 3.2 and 5.8 times lower than that measured for OSB// and OSBT panels, respectively). At the same time, strength and absorbed energy were larger than that exhibited by GWB sheathings (on average, 1.5 and 1.2 times larger, respectively). Some typical load vs. displacement curves, obtained from tests under monotonic tension (Fig. 7(a)) and compression (Fig. 7(b)) loading are presented in Figure 7.

Average values of  $K_e$ ,  $F_u$ ,  $\mu$ , and  $E$  obtained in the case of cyclic tests considering CF and CK protocols are shown in Figure 6 (a)–(d). It is worth to specify that OSBT panels were not subjected to cyclic tests. The comparison about stiffness and strength among CP, OSB// and GWB sheathings results confirms the conclusions drawn in the case of monotonic tests. In fact, from cyclic loading test results it can be observed that CP sheathings have larger stiffness then OSB// and GWB (1.7 and 1.2 times, respectively) and the strength is lower then for OSB// panels (1.5 times) and higher then GWB sheathings (1.7 times). About ductility and absorbed energy, the results seem to confirm the monotonic ones for CP and GWB, in fact CP ductility is 1.7 times lower then GWB ductility while CP sheathings absorbed more energy then GWB panels. On the contrary, the comparison about ductility and absorbed energy between CP and OSB does not confirm the conclusions drawn in the case of monotonic tests. In this case, in fact, CP panels reveal lower ductility (1.2 times) and absorbed larger energy (1.2 times) then OSB// sheathings.

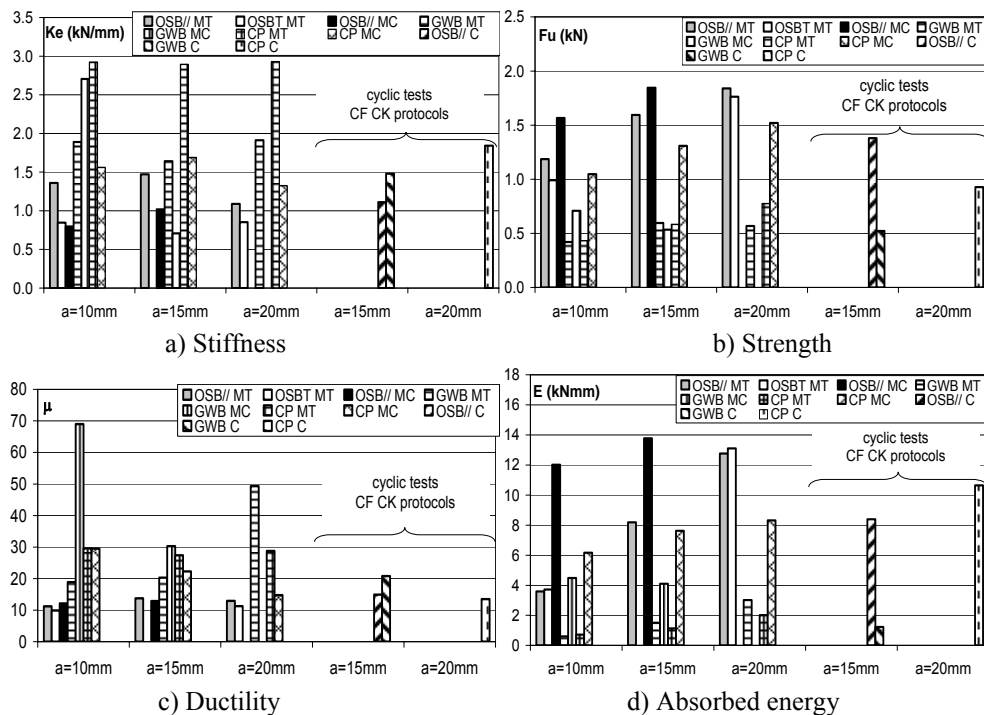


Figure 6: Average values of  $K_e$ ,  $F_u$ ,  $\mu$  and  $E$  obtained during monotonic and cyclic tests

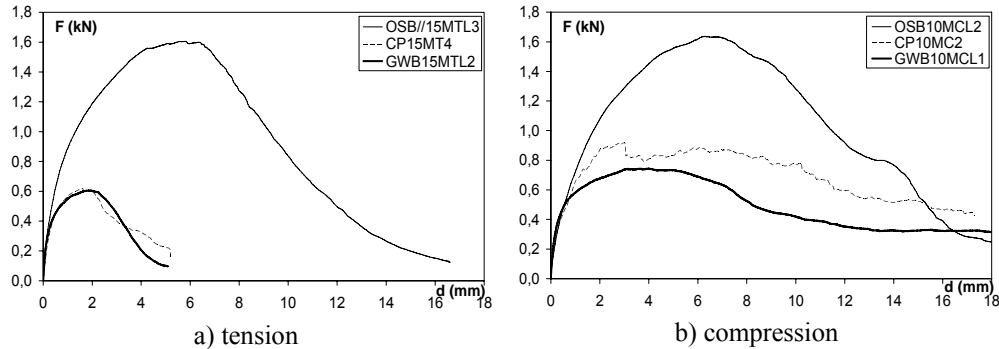


Figure 7: OSB//, GWB and CP experimental response under monotonic loads

#### Effect of the loaded edge distance

As far as the influence of the loaded edge distance ( $a$ ) is concerned, results of monotonic tests on CP sheathings represented in Figure 6 reveal that strength and absorbed energy are increasing with  $a$ . In particular, test results under monotonic tension loading show that an increase of the edge distance from 10 to 20 mm produced an increase of strength of about 1.8 times and an increase of absorbed energy of about 2.8 times. Moreover, when  $a$  was increased the strength and absorbed energy exhibited an almost linear variation. In the case of monotonic compression loading, when the edge distance was increased from 10 to 20 mm strength and absorbed energy increased about 1.5 times. The ductility did not vary significantly when  $a$  was increased in case of tension loads, while it decreases of almost 50% in case of compression loads. Finally, stiffness values varied without any noticeable trend.

Typical load vs. displacement response curves for three different values of the adopted loaded edge distance are shown in Figure 8. Examining this figure, two boundary behaviours can be individuated: (1) shear response is significantly affected by edge failure (E failure mode), for  $a = 10$  mm; (2) shear response is significantly affected by an interaction of tilting and screw pull-through the sheathing failure (T+P failure mode) for  $a = 20$  mm. In particular, the second case can be associated with a better behaviour characterized by larger strength and absorbed energy than the first one.

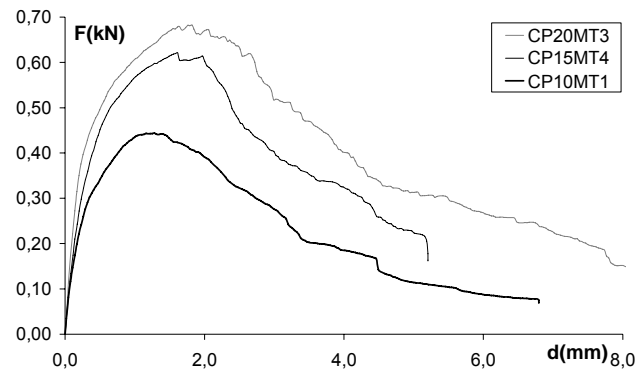


Figure 8: Experimental response of Monotonic Tension tests as function of the loaded edge distance

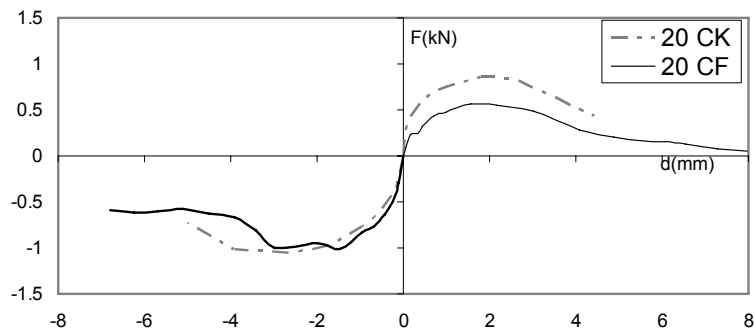


Figure 9: Average back-bone curves

The difference between these boundary behaviours justifies that in the design of shear walls based on theoretical methods, in which the global shear response is evaluated on the basis of a connection's shear response (local response), knowledge of the strength values corresponding to edge and pull-through failure modes is required. As a result of this experimental research, nominal values (experimental average values) of shear strength due to edge failure ( $F_u^{(e)}$ ) and screw pull-through the sheathing failure ( $F_u^{(p)}$ ) are suggested as follows: for 12.5mm thick standard CP sheathing fastened to 1.0 mm thick steel profiles with a  $3.5 \times 25$  mm bugle head self drilling screw:  $F_u^{(e)} = 0.43\text{kN}$  and  $F_u^{(p)} = 0.78\text{kN}$ ; standard deviations were 0.04 for  $F_u^{(e)}$  and 0.10 for  $F_u^{(p)}$ .

### Effect of different cyclic loading protocols

Figure 9 shows the average envelope curves obtained at the first hysteretic loops (envelope obtained considering the maximum value of strength measured at the first loop for each displacement amplitude) and considering the adopted loading protocols (CF, CK) for CP sheathings. For evaluating the effect of cyclic loading on the strength degradation, envelope curves obtained at the second and third hysteretic loops (envelopes obtained considering the maximum value of strength measured for each displacement amplitude at the second and third loop, respectively) have been considered together with the envelope curve obtained considering the first hysteretic loop. Figure 10 shows comparison between the monotonic and cyclic response. In this figure the values of  $K_e$ ,  $F_u$ ,  $\mu$  and  $E$  obtained applying the adopted cyclic loading protocols (CF, CS) are normalized with respect to the values that these parameters assume for the monotonic loading protocol. In particular, values of parameters assumed as representative of monotonic response have been calculated as average values of parameters obtained from monotonic tension (MT) and compression (MC) tests. Examining this figure, it can be noticed that stiffness, strength, absorbed energy and ductility obtained in cyclic tests were lower than those obtained in monotonic tests. In particular, more significant reductions were obtained for  $F_u$  (by 16% and 32% considering CK and CF protocols, respectively) and  $E$  (by 40% and 216% considering CK and CF protocols, respectively). Figure 11 shows representative curves obtained from tests (CP20MT3 vs. CP20CF2), in which monotonic and cyclic experimental response can be directly compared.

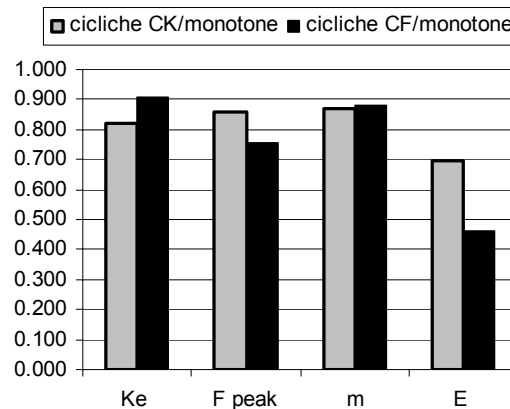


Figure 10: Monotonic vs. cyclic response

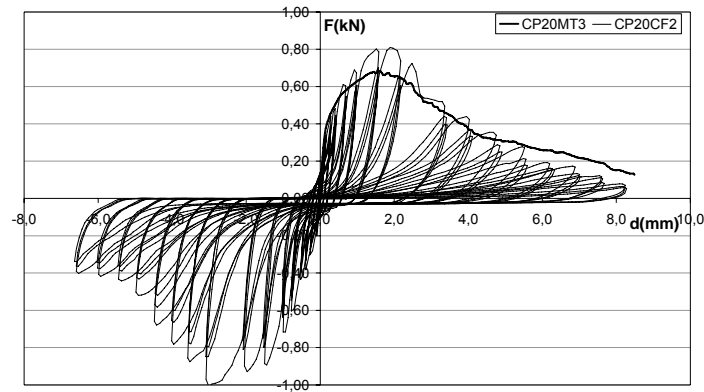


Figure 11: Monotonic vs. cyclic experimental response

## Conclusions

The sheathing strongly influences the shear response of connections. In fact, as showed in the presented paper, the CP sheathing reveals larger stiffness than OSB and GWB panels. Moreover, CP ductility is almost the same of GWB panels and it is larger than that exhibited by OSB. On the contrary, CP reveals less strength and absorbed less energy than OSB even if both are larger than that exhibited by GWB sheathing. The increment of the loaded edge distance produced an increment of strength and absorbed energy with an almost linear variation. The ductility is strongly influenced in case of compression tests, whilst ductility in tension tests and the stiffness varied without any noticeable trend. The suggested nominal strength for the tested CP screw connections (12.5 mm thick standard CP sheathing fastened to 1.0 mm thick steel profiles with a  $3.5 \times 25$  mm screw) is 0.43kN or 0.78kN in case of edge failure or pull-through the sheathing failure, respectively. Comparison between monotonic and cyclic response reveals that cyclic loading produces a reduction of all the parameters (stiffness, strength, ductility and absorbed energy), with a non-negligible reduction of absorbed energy.

## Achievements

Authors acknowledge the Italian companies BPB Italia Spa., TECFI Spa. and GUERRASIO for the furnishing of test specimen components. Specific

acknowledgments are extended to Eng. Pino Campanella for the technical support provided during the laboratory phase and to Eng. Gennaro De Crisci involved in the experimental activity during his Dissertation Thesis.

## References

- AISI. 2002. Cold-formed steel design manual. Washington (DC, USA): American Iron and Steel Institute.
- Della Corte G, Landolfo R, Fiorino L. 2006. Seismic behavior of sheathed cold formed structures: Numerical study. *Journal of Structural Engineering ASCE*; 132(4):558–69.
- EN 1993-1-3. 2005. Eurocode 3: Design of steel structures—Part 1–3: General rules — Supplementary rules for cold formed members and sheeting. Bruxelles (Belgium): European Committee for Standardization.
- EN 300. 1997. Oriented strand boards OSB-definitions, classification and specifications. Bruxelles (Belgium): European committee for standardization.
- Filipsson T. 2002. *Shear walls with double plasterboards — Evaluation of design models*. Licentiate thesis. Luleå (Sweden): Department of Civil and Mining Engineering, Division of Steel Structures, Luleå University of Technology.
- Fulop LA, Dubina D. 2004. Design criteria for seam and sheathing-to-framing connections of cold-formed steel shear panels. In *Proceedings of the 17th international specialty conference on cold-formed steel structures*. p. 743–59.
- Fiorino, L., Della Corte, G., Landolfo, R. 2007. Experimental tests on typical screw connections for cold-formed steel housing. *Engineering Structures*. Elsevier Science. Vol. 29, No. 8, pp. 1761–1773.
- ISO-6308. 1980. Gypsum plasterboard-specification. Geneva (Switzerland): International organization for standardization.
- Landolfo R, Fiorino L, Della Corte G. 2006. Seismic behavior of sheathed coldformed structures: Physical tests. *Journal of Structural Engineering ASCE*; 132(4):570–81.
- Krawinkler H, Parisi F, Ibarra L, Ayoub A, Medina R. 2000. *Development of a testing protocol for wood frame structures*. Report W-02 covering task 1.3.2, CUREE/Caltech wood frame project.
- Okasha AF. 2004. *Performance of steel frame/wood sheathing screw connections subjected to monotonic and cyclic loading*. M.Sc. Thesis. Montreal (Canada): Department of Civil Engineering and Applied Mechanics, McGill University.



